Supporting Information

Antimicrobial and aging properties of Ag-, Ag/Cu- and Ag cluster-doped amorphous carbon coatings produced by magnetron sputtering for space applications

Giuseppe Sanzone[1, 2], Susan Field[1], David Lee[3], Jingzhou Liu[4], Pengfei Ju[4], Minshi Wang[5], Parnia Navabpour[1], Hailin Sun[1], Jinlong Yin[1, (*)], Peter Lievens[2].

[1] Teer Coatings Ltd., West Stone, Droitwich, Worcestershire, WR9 9AS, United Kingdom

[2] Quantum Solid-State Physics, Department of Physics and Astronomy, KU Leuven, B-3001 Leuven, Belgium

[3] Department of Life Sciences, School of Health Sciences, Birmingham City University, Birmingham B15 3TN, United Kingdom

[4] Shanghai Aerospace Equipment Manufacturer, 100 Huaning Road, Minhang, Shanghai 200245, China

[5] School of Metallurgy and Materials, University of Birmingham, B15 2TT, United Kingdom

[(*)] Corresponding author: Dr Jinlong Yin (jinlong.yin@teercoatings.co.uk) Teer Coatings Ltd, West Stone, Droitwich, Worcestershire, WR9 9AS, UK

Grazing-Incidence Small-Angle X-ray Scattering (GISAXS) measurement and data analysis

All measurement were made on a Xenocs Xeuss 2.0 equipped with a Cu K_α source collimated by two sets of Scatterless slits. A Pilatus 300k detector mounted on a translation stage was used to record the scattered signal. Measurements were made with a sample to detector distance of 1.188(5) m giving a 1-82 nm particle size range or a sample to detector distance of 0.540(5) m giving a 1-35 nm particle size range. The distance was calibrated using a silver behenate standard.

1. Measurement procedure and results:

Samples were aligned using the x-ray beam such that the surface of the sample was parallel to the beam. These measurements were focused around the critical angle (≈ 0.2°) for the carbon top layer. Below the critical angle the x-rays would be totally reflected from the surface and above they would start to penetrate the carbon layer. At an angle of 0.3° the scattering from sample A3 was the strongest, so this angle has been used for analysis.

The measured scattering from a 30 minute collection at 0.3° for sample A3, with a sample to detector distance of 1.188(5) m, are shown in Figure S1a. A strong scattering signal from the Ag nanoparticles can be seen from sample A3. The scattering from the Ag particles extends to the right side of the detector so a repeat measurement was made with the detector closer to the sample, i.e. at 0.540(5) m, shown in Figure S1b. This extends the range to larger q values and shows the scattering reducing to a background value.

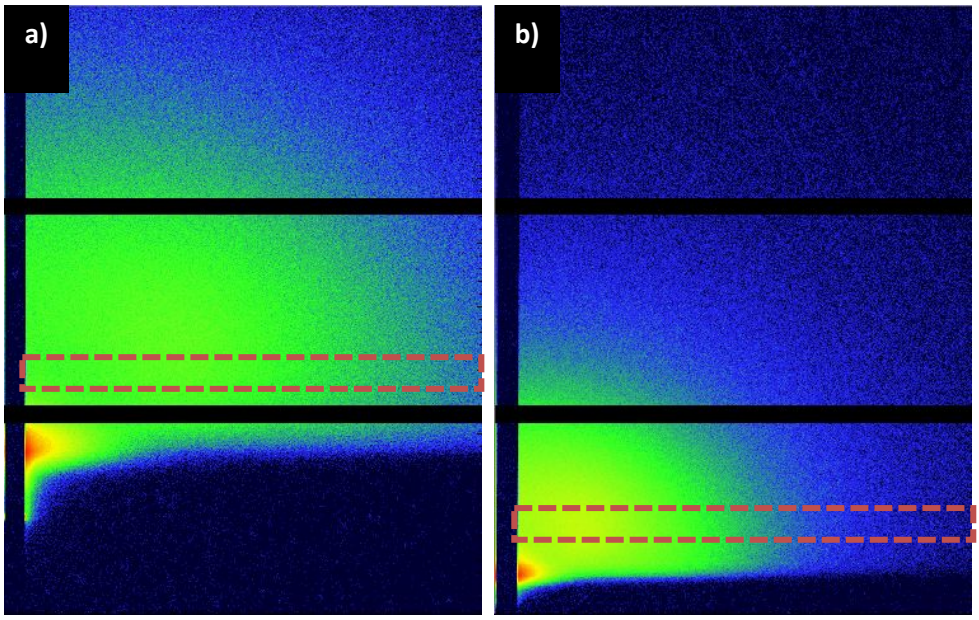

Figure S1: Detector image of sample *A3* for a sample to detector distance of a) 1.188(5) m and b) 0.540(5) m.

2. Analysis

We have measured the scattering parallel to the sample surface so the particle sizes and distributions determined will be in-plane sizes. The scattering has been modelled as spheres with the radius given by a log-normal distribution [1]. For samples *B3* and *A4*, the particles are close enough and concentrated enough that the interaction between them also affects the scattering. This results in a peak in the scattering around 0.1 $Å^{-1}$. A hard sphere interaction model has been used to account for the effect on the scattering from neighbouring particles [2]. The hard sphere interaction models the effects of particles getting close to each other by treating them as a hard sphere with a radius given by R_{HS}. Figure S2 shows R_{HS} in relation to the sphere radius. Both the sphere radius and hard sphere radius are refined with the hard sphere radius constrained to be equal to or larger than the sphere radius. The hard-sphere interaction also refines what volume fraction of space surrounding a particle contains another particle.

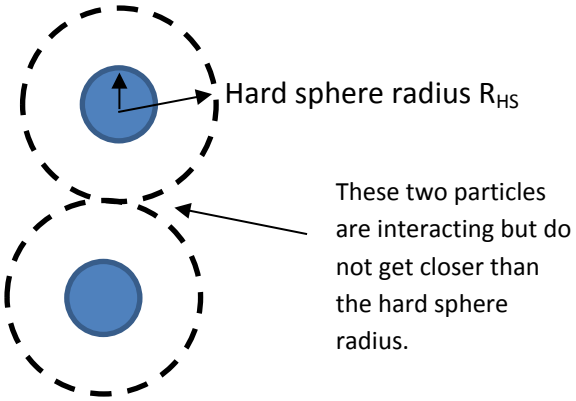

Figure S2: The hard-sphere interaction radius compared to the radius of the particles.

The horizontal scattering signal was extracted from the 2d images by integration within a selected region. The dashed red lines in Figure S1 show the region used for integration for sample *A3*. The size of the region integrated was kept the same for all samples. Integrating the 2d detector image provides a 1d dataset that allows us to plot the scattered intensity versus the scattering vector (q). The 1d data for sample *A3* for the two detector distances, i.e. 1.188(5) m and 0.540(5) m, are plotted in Figures S3a and S3b, respectively. The Ag nanoparticle radii distributions are plotted in Figure S3c, and have been normalised to allow comparisons. The results measured for sample *A3* are consistent for both sample-to-detector distances used.

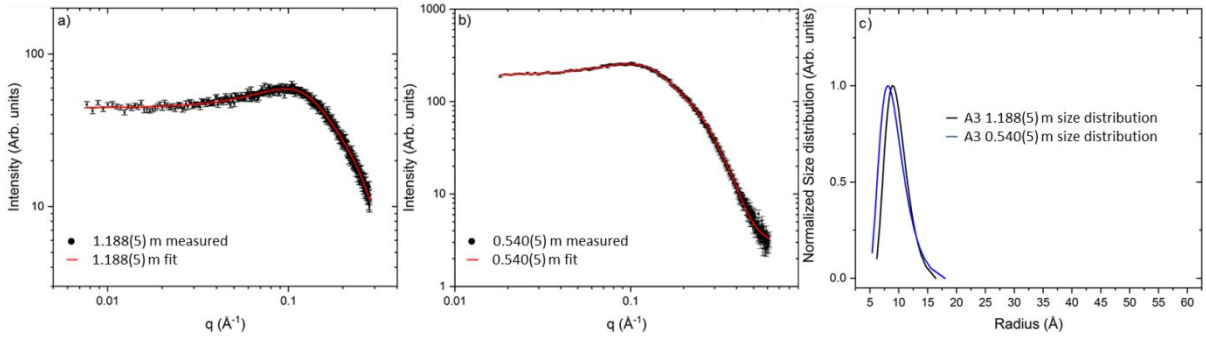

Figure S3: Integration of the signal from the highlighted regions in Fig. S1 for sample *A3* with a sample to detector distance of, respectively, a) 1.188(5) m and b) 0.540(5) m. c) Size distributions of particles for sample *A3* with a sample to detector distance of, respectively, 1.188(5) m (black line) and 0.540(5) m (blue line).

To prevent any scattering signal loss due to the sample-to-detector distance being too high, samples *A1*, *A4*, *B3*, *NP1* and *NP3* were measured with a sample to detector distance of 0.540(5) m.

The particle radii and distribution for the samples *A1*, *A4* and *B3* are shown in Figure S4 and listed in Table S1 along with the hard sphere interaction parameters. The particle size for sample *A1* is very small and gets close to the lower limit for the equipment. For the modelling the minimum size a particle can be is set to 3 Å. The SAXS signal and modelling results for samples *B3* and *A4* are very similar. The radii distributions of the spherical models are compared in Figure 2 of the main article.

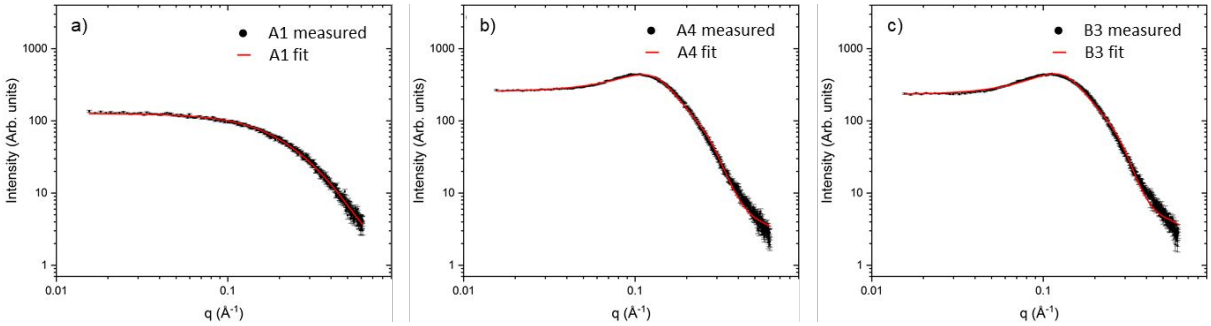

Figure S4: The measured GISAXS response compared for samples a) *A1*, b) *A4* and c) *B3*, with fits to the data given by the red lines.

Table S1: Fit parameters for samples.

Sample	Mean radius/ Å	FWHM/ Å	R_{HS}/ Å	Volume fraction
A1	7	4	-	-
A4	11	6	22	0.13
B3	11	5	22	0.14

Samples *NP1* and *NP3* have been modelled using two populations of spheres. The data and fits are plotted in Figure S5 and listed in table S2. Including the second smaller population of spheres produces a better overall fit to the measured data. The second population of spheres have mean radii of 7 and 9 Å for samples *NP1* and *NP3*, respectively. The size distributions are plotted in Figure 3 in the manuscript for the two sphere population modelling.

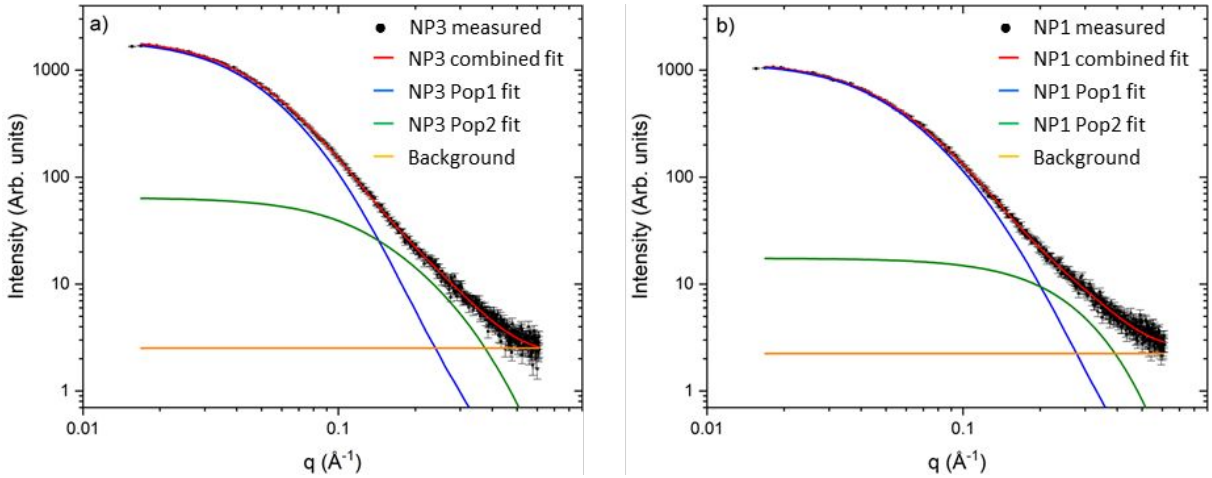

Figure S5: Samples a) *NP3* and b) *NP1* modelled using two particle distributions. The measured data is given by the black squares, the combined fit by the red line, the fit of population 1 by the blue line, the fit of population 2 by the green line and the background by the orange line.

Table S2: Updated fit parameters for carbon-based samples using two particle distributions.

Sample	Population 1		Population 2	
	Mean radius/ Å	FWHM/ Å	Mean radius/ Å	FWHM/ Å
NP1	23	18	7	3
NP3	30	23	9	5

References

1. https://www.sasview.org. [Online]. Available from: https://www.sasview.org/docs/user/qtgui/Perspectives/Fitting/pd/polydispersity.html.

2. https://www.sasview.org. [Online]. Available from: https://www.sasview.org/docs/user/models/hardsphere.html.